

Highly Strained Oxygen-Doped Chiral Molecular Belts of the Zigzag-Type with Strong Circularly Polarized Luminescence

Jia-Hui Chen, Zhi-Yu Jiang, Hai Xiao,* Shuo Tong,* Tan-Hao Shi, Jieping Zhu, and Mei-Xiang Wang

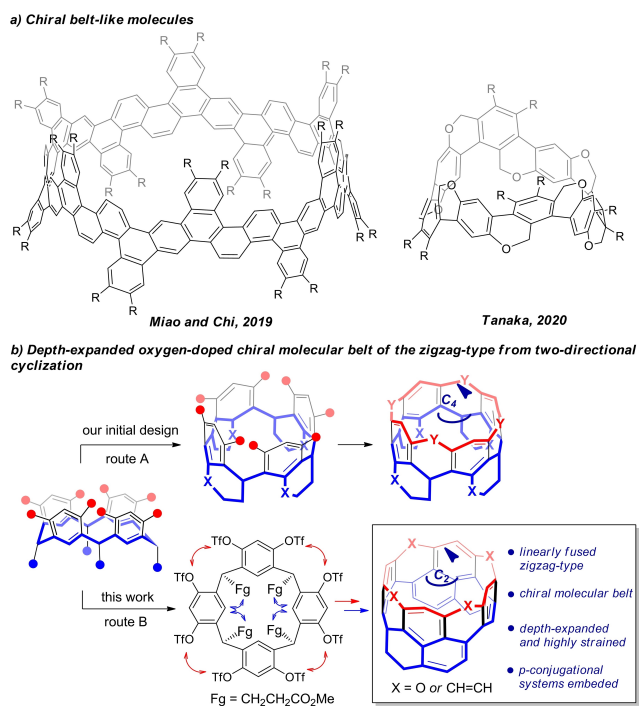
Abstract: Herein we report a two-directional cyclization strategy for the synthesis of highly strained depth-expanded oxygen-doped chiral molecular belts of the zigzag-type. From the easily accessible resorcin[4]arenes, an unprecedented cyclization cascade generating fused 2,3-dihydro-1H-phenalenes has been developed to access expanded molecular belts. Stitching up the fjords through intramolecular nucleophilic aromatic substitution and ring-closing olefin metathesis reactions furnished a highly strained O-doped C₂-symmetric belt. The enantiomers of the acquired compounds exhibited excellent chiroptical properties. The calculated parallelly aligned electric (***μ***) and magnetic (***m***) transition dipole moments are translated to the high dissymmetry factor ($|g_{lum}|$ up to 0.022). This study provides not only an appealing and useful strategy for the synthesis of strained molecular belts but also a new paradigm for the fabrication of belt-derived chiroptical materials with high CPL activities.

Hydrocarbon nanobelts have been fascinating chemistry and materials communities since beltarenes or cyclacenes were proposed by Heilbronner as fictional molecules in 1954^[1] and then as challenging synthetic targets by Vögtle in 1983.^[2] There are three types of belt-shaped hydrocarbon molecules, namely, armchair, zigzag, and chiral ones, depending on the fusion pattern of hexagonal aromatic units. Interesting physical and chemical properties are predicted for these aesthetically appealing structures.^[3-5] Moreover, they are expected to serve as templates to grow structurally well-defined and uniform single-walled carbon nanotubes.

[*] J.-H. Chen, Z.-Y. Jiang, Prof. Dr. H. Xiao, Prof. Dr. S. Tong, Dr. T.-H. Shi, Prof. Dr. M.-X. Wang
Key Laboratory of Bioorganic Phosphorus Chemistry and Chemical Biology (Ministry of Education), Department of Chemistry, Tsinghua University
Beijing 100084 (China)
E-mail: haixiao@tsinghua.edu.cn
tongshuo@mail.tsinghua.edu.cn
Homepage: <http://mascl.group>
Prof. Dr. J. Zhu
Laboratory of Synthesis and Natural Products (LSPN), Institute of Chemical Sciences and Engineering, Ecole Polytechnique Fédérale de Lausanne, EPFL-SB-ISIC-LSPN, BCH5304, 1015 Lausanne (Switzerland)

Significant progress in the synthesis of hydrocarbon molecular belts have been recorded in recent years. Itami and Segawa succeeded in the synthesis of an armchair belt in 2017 by means of multiple intramolecular Yamamoto coupling reactions of a polybrominated macrocyclic precursor,^[6] while Miao and Chi constructed the same type of belts by the Scholl reaction of polyarylated cycloparaphenyls (CPPs) in 2019.^[7] Our group reported in 2020 the synthesis of partially hydrogenated belt[n]arenes by stitching up all fjords of strainless resorcin[n]arene derivatives through multiple intramolecular alkylation^[8] and acylation reactions.^[9] Itami^[10] and Chi^[11] reported independently in 2021 the synthesis of benzannulated [18]cyclacene and [12]cyclacene through iterative Diels–Alder cycloadditions followed by reductive aromatization, a strategy pioneered by Stoddart in the late 1980s.^[12] A similar route has also been utilized by the group of Miao for the synthesis of pyrene-containing zigzag-type belts.^[13] The resurgence of interest in hydrocarbon belts has led to the successful synthesis of other armchair- and zigzag-type belt-like molecules containing various heteroatoms^[14] and non-hexagonal rings.^[15] In stark contrast to the achiral structures, examples of chiral hydrocarbon belts are rare (Scheme 1a). A chiral carbon nanobelt was successfully synthesized by Miao and Chi by the Scholl reaction of a cycloparaphenylene analogue composed of alternate 2,6-naphthalenylene and diarylated 1,4-phenylene segments.^[7] Applying the powerful rhodium(I)-catalyzed [2+2+2] alkyne cyclotrimerization method, Tanaka reported an enantioselective synthesis of the chiral cyclophenylene belts which contain 6H-benzo[c]chromene-fused ring units (Scheme 1a). The resulting chiral belts have also been shown by the authors to have interesting chiroptical properties.^[16] To the best of our knowledge, the chiral belts bearing linearly fused zigzag-type structures remain unknown. In particular, the construction of depth-expanded chiral belts with high strain and rigidity are very appealing but unexplored.

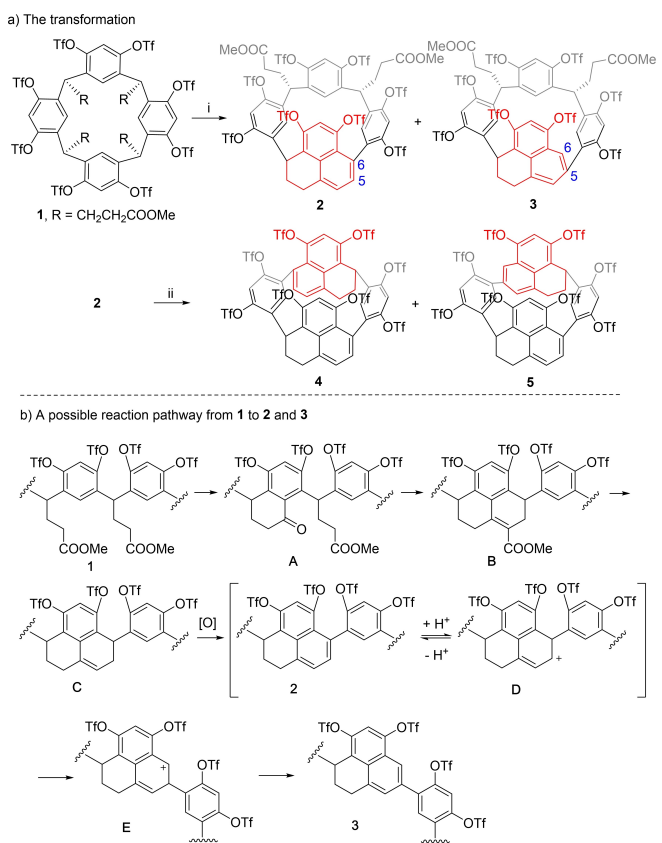
Herein, we report a two-directional cyclization strategy for the synthesis of depth-expanded oxygen-doped chiral molecular belts of the zigzag-type. Their multiple-stranded macrocyclic structure gives the belt molecules a high degree of rigidity and strain. Our design was based on the formation of a belt by stitching up four fjords of resorcin[4]arenes and the growth of the edge by intramolecular cyclization between aromatic rings and appended functional groups of the resorcin[4]arene. The fjord-stitching-up strategy offers the advantages not only because the starting materials such as resorcinarenes^[17] and calixarenes^[18] are readily available,



Scheme 1. Design of depth-expanded oxygen-doped chiral molecular belts of the zigzag-type.

but it also allows the introduction of functional groups into belt edges either during the fjord-bridging steps or simply using properly functionalized macrocyclic precursors. The functional groups installed on the edges would provide useful handles for the fabrication of depth-expanded belts. We envisioned that fourfold Friedel–Crafts acylation and subsequent chemical transformations would produce linearly fused zigzag-type chiral belt compounds with C_4 -symmetry (Route A, Scheme 1b). Surprisingly, we discovered that the acylation reaction of resorcinarene derivatives afforded a 2,3-dihydro-1*H*-phenalene-bearing macrocycle with larger π -conjugational systems (Route B, Scheme 1b). The subsequent fjord-stitching reactions and transformations enabled the synthesis of chiral depth-expanded zigzag-type belt-like molecules with high strain and rigidity. The chromophores generated during belt formation impart excellent chiroptical properties to the chiral belts.

A 2,8,14,20-tetrakis(methoxycarbonylethyl)-substituted resorcin[4]arene derivative **1** was prepared from resorcinol following literature procedure (see the Supporting Information).^[17] Heating a solution of **1** in a mixture of trifluoroacetic acid anhydride $[(CF_3CO)_2O]$, trifluoromethanesulfonic acid (TfOH) and methanol (v/v/v, 50/50/3) afforded two products, whose structures were determined to be **2** and **3** on the basis of detailed spectroscopic data analysis (Scheme 2a, Supporting Information). Notably, **3** is the isomer of **2** with a biaryl bond migrated from the C(6) to the C(5) position. Increasing the reaction temperature and the amount of $(CF_3CO)_2O$ to 60 % afforded the products **2** and **3** in yields of 31 % and 11 %, respectively. Subsequently, heating a solution of compound **2** in a mixture of



Scheme 2. a) Synthesis of **2–5**. Conditions: i, **1**, $(CF_3CO)_2O/TfOH/MeOH$ (v/v/v, 60/40/3), 90°C, 15 h, **2(3)**, 31% (11%); ii, **2**, $(CF_3CO)_2O/TfOH/MeOH$ (v/v/v, 70/30/3), 140°C, 10 h, **4(5)**, 32% (32%). b) A possible reaction pathway converting **1** into **2** and **3**.

$(CF_3CO)_2O$, TfOH, and MeOH (v/v/v, 70/30/3) at 140°C for 10 h provided a separable mixture of macrocycles **4** and **5** (ratio 1:1) in 64 % yield. A possible reaction pathway converting **1** into **2** and **3** is depicted in Scheme 2b (see the Supporting Information for details). The intramolecular Friedel–Crafts acylation of **1** followed by a cross-Claisen condensation of the resulting tetralone derivative **A** would afford **B**. Hydrolysis of the latter followed by decarboxylation would furnish **C**. Oxidative aromatization of **C** would lead to the formation of **2**. Under the acidic reaction conditions, compound **2** would undergo aryl migration to afford **3** via intermediates **D** and **E** (see Supporting Information, Figure S2). X-ray structural analysis indicated that compound **4** contains a C_2 axis of rotation rather than a mirror plane (Figure 1 and Figure S20).^[19] In other words, the two newly formed 2,3-dihydro-1*H*-phenalene segments in **4** are distally positioned.

The favorable boat or flattened cone conformation of **4** as illustrated in Figure 1 prompted us to exploit its application in the construction of C_2 -symmetric belts (Scheme 3). Heating a *N,N*-dimethylformamide (DMF) solution of **4** in the presence of K_3PO_4 (6 equiv) and H_2O (6 equiv) at 100°C afforded a dioxo-linked half-belt product **6** through a double intramolecular nucleophilic aromatic substitution reaction (S_NAr ; Scheme 3). The attempted syn-

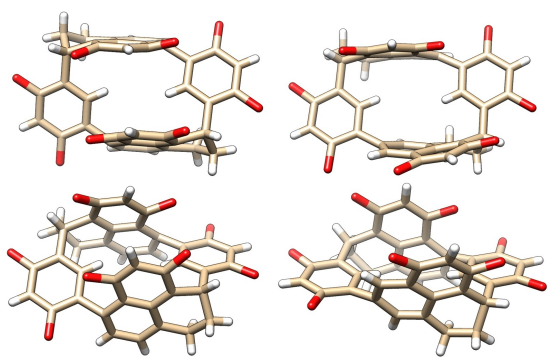
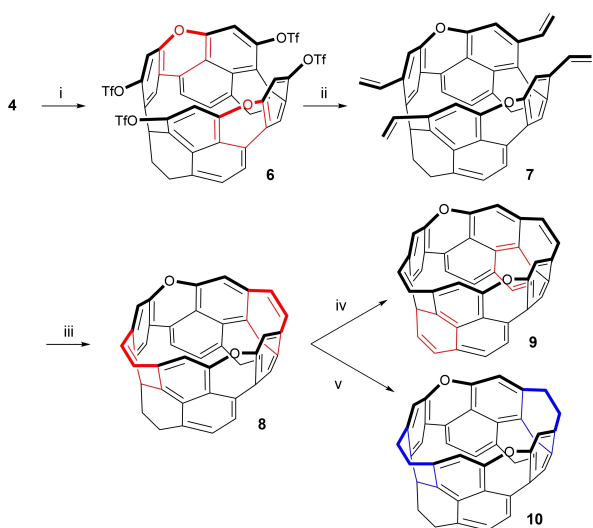


Figure 1. X-ray molecular structures of **4** (left) and **5** (right) with top (top) and side (bottom) views. Solvents and Tf moieties are omitted for clarity.



Scheme 3. Synthesis of belts **8–10**. Conditions: i, K_3PO_4 (6 equiv), H_2O (6 equiv), DMF, $100^\circ C$, 3 h, 31%; ii, $CH_2=CHSnBu_3$ (8 equiv), $Pd-(PPh_3)_2Cl_2$ (1 equiv), $LiCl$ (20 equiv), DMF, under N_2 , $80^\circ C$, 18 h, 52%; iii, Grubbs-II catalyst (0.5 equiv), DCM, under N_2 , reflux, 12 h, 65%; iv, DDQ (4 equiv), PhMe, reflux, 12 h, 64%; v, H_2 (1 atm), Pd/C (10% w/w), $EtOAc$, RT, 4 h, 94%.

thesis of a tetraoxa-bridged molecular belt from **4** and from **6** under forcing conditions was unsuccessful because of the substantial ramp-up of molecular strain.^[20] We then focused on the closure of two fjords of **6** by forming seven-membered rings. To our delight, the palladium-catalyzed Stille cross-coupling reaction of **6** with a vinyltin reagent proceeded efficiently to afford tetravinyl-substituted half-belt product **7**. Dual olefin metathesis promoted by Grubbs-II catalyst generated a dioxia-embedded zigzag-type molecular belt **8** in 65% yield. To diversify the belt structures and also to shed light on the structural effect on chiroptical property (see below), the oxidation and reduction reactions of **8** were investigated. Treatment of **8** with 1,2-dichloro-4,5-dicyanobenzoquinone (DDQ) in refluxing toluene generated belt **9** in 64% yield, while the catalytic hydrogenation of **8** delivered product **10** almost quantitatively (Scheme 3).

Racemic samples were resolved efficiently using a chiral HPLC method (Figures S5–S19). The absolute configuration of enantiopure compounds **P-4**, **M-6**, **P-8**, **P-9**, **M-10** was determined unambiguously by X-ray diffraction methods.^[19] The molecular structures of racemic products **6**, **8**, **9**, and enantiopure **M-10** are shown in Figure 2 and Figures S22, S24, S26, and S28. All compounds **8–10** give similar highly strained belt structures. The oval molecular shapes of the compounds arise from the two sp^3 -hybridized carbon atoms connecting the conjugated π -systems like cornerstones. The distances between two oxygen atoms (minor axis) and between the centroids of the upper-rim C–C bonds of seven-membered rings (major axis) are in the range of 5.379–6.335 Å and 7.976–8.868 Å, respectively, depending on the saturation of the molecules. In comparison to the half belt molecule **6**, formation of the belt structure **8** led to an increase in the distance between the two oxygen atoms to 6.316 Å. Introduction of a double bond into the six-membered ring through oxidation resulted in the slight expansion of the cavity (**9** vs **8**). Increasing eccentricity was evident for compound **10** containing a 2,3-dihydro-1*H*-phenalene moiety. In all cases, the seven-membered rings adopt a boat conformation to minimize the strain of belts, with relatively large out-of-plane deformation of the naphthalene rings (see Supporting Information).^[21] The rigid belt structures also forced the $-\text{CH}_2\text{CH}_2-$ group in **8** and **10** to adopt a nearly eclipsed conformation, increasing further the strain in the belts. It is worth stressing that the zigzag-type belt molecules obtained in the current study are greater in height than previously reported ones^[4] thanks to the growth of fused rings on the edge.

The strain energies of compounds **8–10** were calculated by a literature method (Supporting Information).^[22,23] The strain energy of belt **8** was found to be 59.6 kcal mol^{-1} . The introduction of extra carbon–carbon double bonds on the lower rim increases considerably the strain energy of **9** to 67.6 kcal mol^{-1} while a slightly decreased strain energy of 53.0 kcal mol^{-1} was computed for **10** after double bonds on the upper rim of **8** were hydrogenated. The buildup of strain in the formation of these belts is clear, as the strain energy of macrocycle **4**, the precursor of these belts, is calculated to be only 6.4 kcal mol^{-1} .

The highly strained chiral zigzag-type belt molecules with varied π -conjugation systems prompted us to investigate their photophysical and chiroptical properties, one of the important aspects of inherently chiral compounds.^[24–27] The UV/Vis absorption and fluorescence emission spectra of belts **8–10** in toluene are shown in Figure 3. For comparison, the spectra of half-belt **6** and macrocycle **4** are also included. All compounds gave absorption bands in the range of 310 to 430 nm. As expected, a bathochromic shift in absorption bands occurred from **8** to **9** due to the increased π -conjugation. Interestingly, belt **10** with a less extended conjugation system than **8** also displayed red-shifted absorption bands, resulting presumably from the increased planarity of the conjugated aromatic segment in **10**. This is in agreement with the structural variation observed in their X-ray structures (Figure 2). Half-belt **6** and belt **10** have a similar benzo[*kl*]xanthene fragment. However, their absorp-

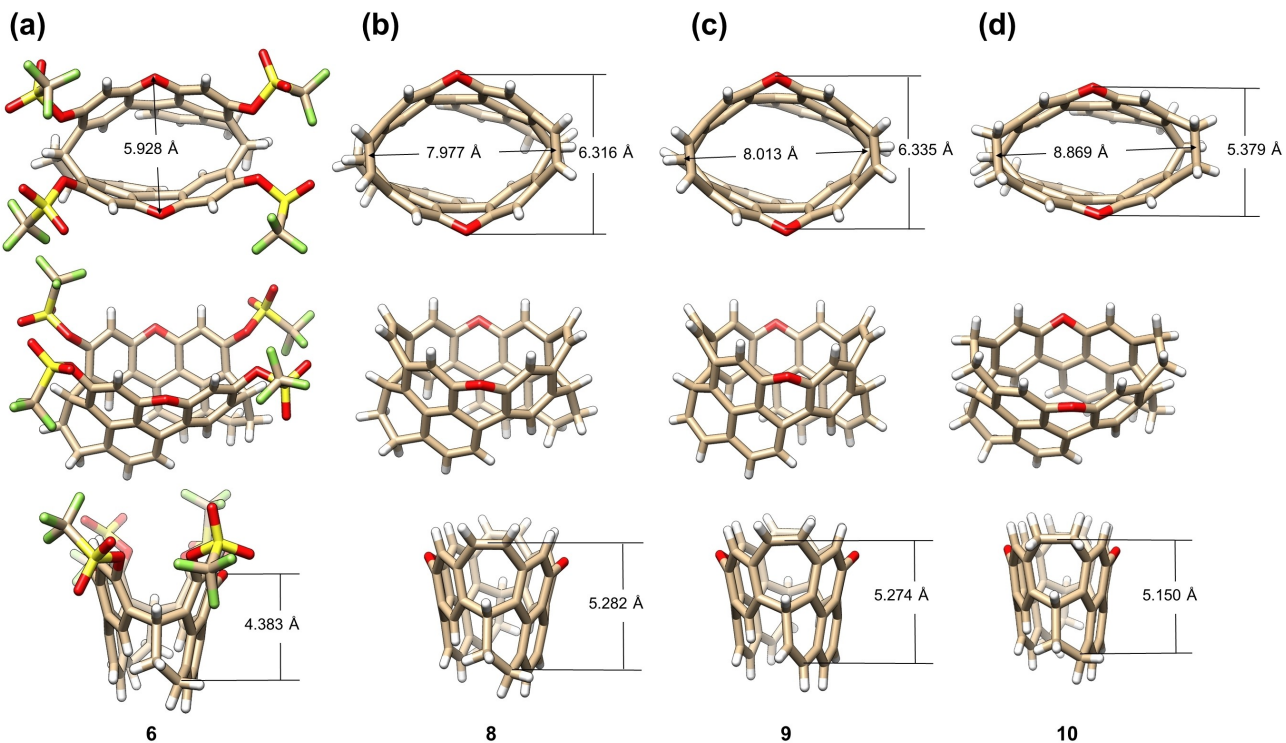


Figure 2. X-ray molecular structures of a) half belt (\pm)-6, belts b) (\pm)-8, c) (\pm)-9, and d) M-10 with top (top) and side (middle and bottom) views.

tion bands differ substantially in shapes and intensities. For example, half-belt **6** exhibited one main band at 358 ($\epsilon=9700 \text{ M}^{-1} \text{ cm}^{-1}$) and a shoulder band at 394 nm ($\epsilon=5900 \text{ M}^{-1} \text{ cm}^{-1}$) while belt **10** showed two main bands at 356 ($\epsilon=14500 \text{ M}^{-1} \text{ cm}^{-1}$) and 388 nm ($\epsilon=13400 \text{ M}^{-1} \text{ cm}^{-1}$). Having the smallest conjugation system, macrocycle **4** gave absorption bands centered at 310 nm. Under UV irradiation, belt compounds **8–10** along with the half-belt **6** gave a fluorescence emission band at 458–480 nm. The emission band of macrocycle **4** appeared, however, at a much shorter wavelength (384 nm). Noticeably, the fluorescence quantum yield (Φ_f) decreased in the order of **9** (0.20) $>$ **8** (0.16) $>$ **10** (0.12) $>$ **6** (0.07) $>$ **4** (0.04) following the order of the molecular rigidity and flexibility.

As illustrated in Figure 3a, complementary circular dichroism (CD) spectra corresponding to the enantiopodes of compounds were observed. Belts **M-8–10** and half-belt **M-6** showed the first noteworthy positive Cotton effects at 413 nm, 443 nm, 420 nm and 388 nm, respectively. By contrast, a very weak Cotton effect was observed for macrocycle **4**. The enantiomers of belts **8–10**, half-belt **6**, and macrocycle **4** also showed perfect mirror images in their CPL spectra and g_{lum} plots. In accord with fluorescence emission spectra, CPL signals were red-shifted from macrocycle **4** to half-belt **6**, and to belt molecules **8–10**. Most remarkably, the CPL intensities were dramatically enhanced from the macrocycle and half-belt to the belts, with the anisotropy dissymmetry factors ($|g_{\text{lum}}|$) changing from 0.001 (**4**) to 0.007 (**6**), and 0.015–0.022 for belts **8–10** (Figure 3b).

The dissymmetry factors can be calculated by the simplified equation $g_{\text{lum}}=4\cos\theta|\mathbf{m}|/|\boldsymbol{\mu}|$, wherein $\boldsymbol{\mu}$, \mathbf{m} , and θ

represent the electric and magnetic transition dipole moments and the angle between them, respectively.^[27a,e,28] To shed light on the chiroptical properties of the belts ($|g_{\text{lum}}|$ up to 0.022) and especially the effects of structure on CPL, an in-depth TDDFT study was performed at the PBE0/6-31G(d) level (Supporting Information). Computational results including $\boldsymbol{\mu}$, \mathbf{m} , and θ values are summarized in Figure 3c,d. The theory-predicted dissymmetry factors ($|g_{\text{lum}}|$) of **4**, **6**, **8–10** for the $S_1 \rightarrow S_0$ transition were in good agreement with the experimental results (Figure 3d). The differences in both the electric and magnetic transition dipole moments ($\boldsymbol{\mu}$ and \mathbf{m}) for belts **8–10** and half-belt **6** was small. However, the angles between $\boldsymbol{\mu}$ and \mathbf{m} differed considerably from belt to belt, and particularly from belt to half-belt and macrocycle. For example, the orientation of $\boldsymbol{\mu}$ and \mathbf{m} in highly stained and rigid belt molecule **9** was parallel with the C_2 -axis of the molecule, leading to a maximum $\cos\theta$ value of 1. A small angle between $\boldsymbol{\mu}$ and \mathbf{m} (25°) was also obtained for belt **8**. As a result, high $|g_{\text{lum}}|$ values were predicted for rigid belts **8** and **9**. A larger θ (a small $\cos\theta$ value) is the major factor to bring about the decrease of $|g_{\text{lum}}|$ in the less rigid belt **10** and flexible half-belt **6**. In the case of macrocycle **4**, a further increased angle between $\boldsymbol{\mu}$ and \mathbf{m} (84°) together with high electric transition dipole moment resulted in the drastic decrease of $|g_{\text{lum}}|$ to 0.001. Overall, it was the combination of (i) the conjugated belt structure, (ii) C_2 -symmetry, and (iii) high molecular rigidity that contributed to the strong circularly polarized luminescence of our belts.

In conclusion, we presented a practical synthesis of depth-expanded linearly fused oxygen-doped chiral molec-

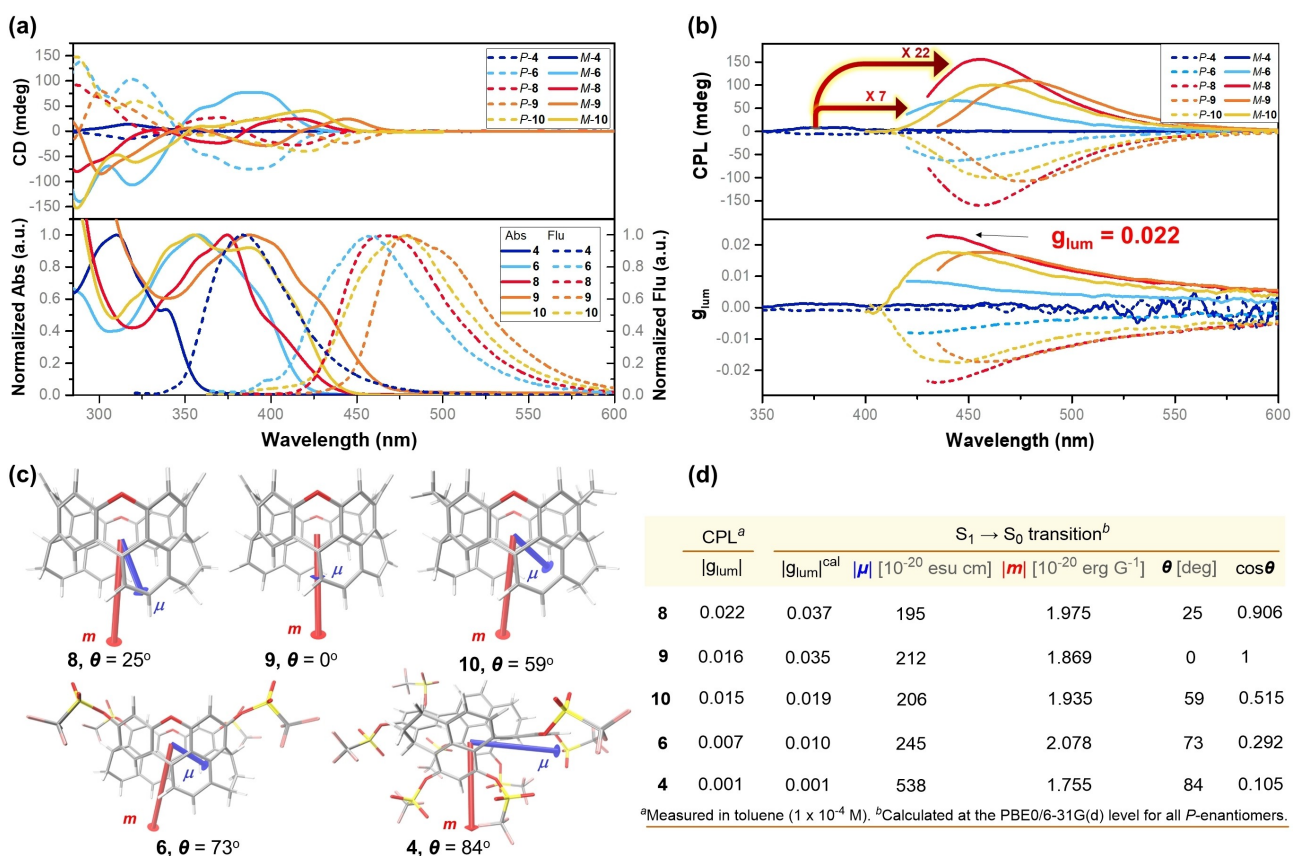


Figure 3. a) Room temperature UV/Vis absorption, emission, and CD spectra of **4**, **6**, **8-10** in toluene. b) CPL emission spectra and luminescence dissymmetry factors of **4**, **6**, **8-10** in toluene (1 × 10⁻⁴ M). c) TD-DFT calculated electric (μ , in blue) and magnetic (m , in red) transition dipole moments for the S₁ → S₀ transitions for all P-enantiomers. For clarity, the length of the m and μ is amplified 8 and 4 times, respectively. d) Summary of the CPL properties of **4**, **6**, **8-10**.

ular belts of the zigzag-type from inexpensive and readily available resorcinol. Growth of fused rings at the lower rim of resorcin[4]arene derivatives followed by closure of fjords at the upper rim characterized our synthetic strategy. We have also demonstrated that the resulting highly strained chiral belts exhibit excellent CPL activities with $|g_{lum}|$ up to 0.022. This work would open a new avenue to construct depth-expanded chiral hydrocarbon molecular belts and could stimulate further development in the fabrication of novel chiroptical materials.

Acknowledgements

We thank the National Natural Science Foundation of China (21920102001, 22050005, 22171160) for financial support. We thank Prof. Lei Jiao and Prof. Wei Jiang for helpful discussions and suggestions.

Conflict of Interest

The authors declare no conflict of interest.

Data Availability Statement

The data that support the findings of this study are available in the Supporting Information of this article.

Keywords: Chirality · Circularly Polarized Luminescence · Molecular Belts · Resorcin[4]Arenes

- [1] E. Heilbronner, *Helv. Chim. Acta* **1954**, 37, 921–935.
- [2] F. Vögtle, A. Schröder, D. Karbach, *Angew. Chem. Int. Ed. Engl.* **1991**, 30, 575–577; *Angew. Chem.* **1991**, 103, 582–584.
- [3] K. Y. Cheung, Y. Segawa, K. Itami, *Chem. Eur. J.* **2020**, 26, 14791–14801.
- [4] T.-H. Shi, M.-X. Wang, *CCS Chem.* **2020**, 2, 916–931.
- [5] Q.-H. Guo, Y. Qiu, M.-X. Wang, J. F. Stoddart, *Nat. Chem.* **2021**, 13, 402–419.
- [6] a) G. Povie, Y. Segawa, T. Nishihara, Y. Miyauchi, K. Itami, *Science* **2017**, 356, 172–175; b) G. Povie, Y. Segawa, T. Nishihara, Y. Miyauchi, K. Itami, *J. Am. Chem. Soc.* **2018**, 140, 10054–11059.
- [7] K. Y. Cheung, S.-J. Gui, C.-F. Deng, Z.-F. Liu, L.-F. Chi, Q. Miao, *Chem* **2019**, 5, 838–847.
- [8] a) T.-H. Shi, Q.-H. Guo, S. Tong, M.-X. Wang, *J. Am. Chem. Soc.* **2020**, 142, 4576–4580; b) T.-H. Shi, S. Tong, M.-X. Wang, *Angew. Chem. Int. Ed.* **2020**, 59, 7700–7705; *Angew. Chem.* **2020**, 132, 7774–7779.

- [9] Y. Zhang, S. Tong, M.-X. Wang, *Angew. Chem. Int. Ed.* **2020**, 59, 18151–18155; *Angew. Chem.* **2020**, 132, 18308–18312.
- [10] K. Y. Cheung, K. Watanabe, Y. Segawa, K. Itami, *Nat. Chem.* **2021**, 13, 255–259.
- [11] Y. Han, S. Q. Dong, J. W. Shao, W. Fan, C. Y. Chi, *Angew. Chem. Int. Ed.* **2021**, 60, 2658–2662; *Angew. Chem.* **2021**, 133, 2690–2694.
- [12] F. H. Kohnke, A. M. Z. Slawin, J. F. Stoddart, D. J. Williams, *Angew. Chem. Int. Ed. Engl.* **1987**, 26, 892–894; *Angew. Chem.* **1987**, 99, 941–943.
- [13] H. Chen, S. J. Gui, Y. Q. Zhang, Z. F. Liu, Q. Miao, *CCS Chem.* **2020**, 2, 613–619.
- [14] a) M.-L. Tan, Q.-H. Guo, X.-Y. Wang, T.-H. Shi, Q. Zhang, S.-K. Hou, S. Tong, J. You, M.-X. Wang, *Angew. Chem. Int. Ed.* **2020**, 59, 23649–23658; *Angew. Chem.* **2020**, 132, 23857–23866; b) M. Xie, S. Tong, M.-X. Wang, *CCS Chem.* **2023**, 5, 117–123; c) S. Nishigaki, Y. Shibata, A. Nakajima, H. Okajima, Y. Masumoto, T. Osawa, A. Muranaka, H. Sugiyama, A. Horikawa, H. Uekusa, H. Koshino, M. Uchiyama, A. Sakamoto, K. Tanaka, *J. Am. Chem. Soc.* **2019**, 141, 14955–14960; d) J. Wang, Q. Miao, *Org. Lett.* **2019**, 21, 10120–10124; e) J. Xie, X. Li, S. Wang, A. Li, L. Jiang, K. Zhu, *Nat. Commun.* **2020**, 11, 3348; f) S. Wang, J. Yuan, J. Xie, Z. Lu, L. Jiang, Y. Mu, Y. Huo, Y. Tsuchido, K. Zhu, *Angew. Chem. Int. Ed.* **2021**, 60, 18443–18447; *Angew. Chem.* **2021**, 133, 18591–18595.
- [15] a) Y. Li, Y. Segawa, A. Yagi, K. Itami, *J. Am. Chem. Soc.* **2020**, 142, 12850–12856; b) J. N. Smith, N. T. Lucas, *Chem. Commun.* **2018**, 54, 4716–4719; c) X.-S. Du, D.-W. Zhang, Y. Guo, J. Li, Y. Han, C.-F. Chen, *Angew. Chem. Int. Ed.* **2021**, 60, 13021–13028; *Angew. Chem.* **2021**, 133, 13131–13138; d) Q. Zhang, Y.-E. Zhang, S. Tong, M.-X. Wang, *J. Am. Chem. Soc.* **2020**, 142, 1196–1199; e) Y.-E. Zhang, S. Tong, M.-X. Wang, *Org. Lett.* **2021**, 23, 7259–7263; f) B. Esser, F. Rominger, R. Gleiter, *J. Am. Chem. Soc.* **2008**, 130, 6716–6717; g) B. Esser, A. Bandyopadhyay, F. Rominger, R. Gleiter, *Chem. Eur. J.* **2009**, 15, 3368–3379; h) F. Zhang, X.-S. Du, D.-W. Zhang, Y.-F. Wang, H.-Y. Lu, C.-F. Chen, *Angew. Chem. Int. Ed.* **2021**, 60, 15291–15295; *Angew. Chem.* **2021**, 133, 15419–15423; i) J. Zhu, Y. Han, Y. Ni, S. Wu, Q. Zhang, T. Jiao, Z. Li, J. Wu, *J. Am. Chem. Soc.* **2021**, 143, 14314–14321.
- [16] J. Nogami, Y. Tanaka, H. Sugiyama, H. Uekusa, A. Muranaka, M. Uchiyama, K. Tanaka, *J. Am. Chem. Soc.* **2020**, 142, 9834–9842.
- [17] P. Timmerman, W. Verboom, D. N. Reinhoudt, *Tetrahedron* **1996**, 52, 2663–2704.
- [18] a) C. D. Gutsche, in *Calixarenes*, Royal Society of Chemistry: Cambridge, U. K., **1989**; b) P. Neri, J. L. Sessler, M.-X. Wang in *Calixarenes and Beyond*, Springer, Switzerland, **2016**.
- [19] Deposition numbers 2179656 (for **P-4**), 2179653 (for **rac-5**), 2179654 (for **rac-6**), 2179658 (for **M-6**), 2179657 (for **rac-8**), 2179655 (for **P-8**), 2179659 (for **rac-9**), 2179660 (for **P-9**) and 2179661 (for **M-10**) contain the supplementary crystallographic data for this paper. These data are provided free of charge by the joint Cambridge Crystallographic Data Centre and Fachinformationszentrum Karlsruhe Access Structures service.
- [20] Calculated strain energy of tetraoxa-bridged molecular belt is 96.6 kcal mol⁻¹ (cf Supporting Information for details).
- [21] S. Biswas, Z. A. Tabasi, L. N. Dawe, Y. Zhao, G. J. Bodwell, *Org. Lett.* **2022**, 24, 5009–5013.
- [22] T.-H. Shi, S. Tong, L. Jiao, M.-X. Wang, *Org. Mater.* **2020**, 2, 300–305.
- [23] a) P. George, M. Trachtman, C. W. Bock, A. M. Brett, *J. Chem. Soc. Perkin Trans. 2* **1976**, 1222–1227; b) S. E. Wheeler, K. N. Houk, P. V. R. Schleyer, W. D. Allen, *J. Am. Chem. Soc.* **2009**, 131, 2547–2560; c) Y. Segawa, H. Omachi, K. Itami, *Org. Lett.* **2010**, 12, 2262–2265.
- [24] E. M. Sánchez-Carnerero, A. R. Agarrabeitia, F. Moreno, B. L. Maroto, G. Müller, M. J. Ortiz, S. de la Moya, *Chem. Eur. J.* **2015**, 21, 13488–13500.
- [25] J.-T. Li, L.-X. Wang, D.-X. Wang, L. Zhao, M.-X. Wang, *J. Org. Chem.* **2014**, 79, 2178–2188.
- [26] S. Tong, J.-T. Li, D.-D. Liang, Y.-E. Zhang, Q.-Y. Feng, X. Zhang, J. Zhu, M.-X. Wang, *J. Am. Chem. Soc.* **2020**, 142, 14432–14436.
- [27] For the synthesis of chiral CPP-derived nanotubes and analogues with excellent chiroptical performances, see: a) S. Sato, A. Yoshii, S. Takahashi, S. Furumi, M. Takeuchi, H. Isobe, *Proc. Natl. Acad. Sci. USA* **2017**, 114, 13097–13101; b) J. Wang, G. Zhuang, M. Chen, D. Lu, Z. Li, Q. Huang, H. Jia, S. Cui, X. Shao, S. Yang, P. Du, *Angew. Chem. Int. Ed.* **2020**, 59, 1619–1626; *Angew. Chem.* **2020**, 132, 1636–1643; c) S. Hitosugi, W. Nakanishi, T. Yamasaki, H. Isobe, *Nat. Commun.* **2011**, 2, 492; d) K. Kogashi, T. Matsuno, S. Sato, H. Isobe, *Angew. Chem. Int. Ed.* **2019**, 58, 7385–7389; *Angew. Chem.* **2019**, 131, 7463–7467; e) T. M. Fukunaga, C. Sawabe, T. Matsuno, J. Takeya, T. Okamoto, H. Isobe, *Angew. Chem. Int. Ed.* **2021**, 60, 19097–19101; *Angew. Chem.* **2021**, 133, 19245–19249; f) X. Zhang, H. Liu, G. Zhuang, S. Yang, P. Du, *Nat. Commun.* **2022**, 13, 3543; g) J. Wang, H. Shi, S. Wang, X. Zhang, P. Fang, Y. Zhou, G.-L. Zhuang, X. Shao, P. Du, *Chem. Eur. J.* **2022**, 28, e202103828.
- [28] F. S. Richardson, J. P. Riehl, *Chem. Rev.* **1977**, 77, 773–792.

Manuscript received: February 5, 2023

Accepted manuscript online: February 17, 2023

Version of record online: March 3, 2023